Is a Transition State Planar or Nonplanar in Oxidative Additions of C−H, Si−H, C−C, and Si−C σ-Bonds to $Pt(PH_3)_2$? A Theoretical Study

Shigeyoshi Sakaki,*,† Nobuteru Mizoe,† Yasuo Musashi,‡ Bishajit Biswas,† and Manabu Sugimoto†

Department of Applied Chemistry and Biochemistry, Faculty of Engineering, Kumamoto University, Kurokami, Kumamoto 860-8555, Japan, and Information Processing Center, Kumamoto University, Kurokami, Kumamoto 860-8555, Japan

Received: April 17, 1998

A theoretical study of oxidative additions of $H-CH_3$, CH_3-CH_3, $H-SiR_3$, and SiR_3-CH_3 (R=H, Cl, or Me) to $Pt(PH_3)_2$ was carried out with ab initio MO/MP2-MP4SDQ, CCD, and CCSD methods. The oxidative addition reactions of C−H and Si−H σ-bonds occur through a planar transition state (TS) structure, in accordance with the expectation from an orbital interaction diagram. However, the oxidative addition reactions of CH_3-CH_3 and SiH_3-CH_3 take place through a nonplanar TS structure, unexpectedly; the dihedral angle δ between PtP_2 and PtXC planes (X = C or Si) is about 70° for X = Si and about 80° for X = C. Intrinsic reaction coordinate calculation of the SiH_3-CH_3 oxidative addition clearly indicated that this nonplanar TS is smoothly connected to the planar product on the singlet surface. The dihedral angle δ at the TS is larger in the $SiMe_3-CH_3$ and $SiCl_3-CH_3$ oxidative additions than that in the SiH_3-CH_3 oxidative addition. Electron distribution in the TS and effects of bulky substituent on the dihedral angle suggest that not an electronic factor but a steric factor is responsible for the nonplanar TS structure of the C−C and Si−C oxidative addition reactions.

Introduction

Oxidative addition reactions of H−H, C−H, Si−C, and Si−Si σ-bonds to transition metal complexes are of considerable importance in organometallic reactions, since transition metal hydride, alkyl, and silyl complexes formed through these oxidative addition reactions are potentially useful as an active species of catalytic reactions.[1] In this regard, many theoretical studies have been carried out on oxidative addition and reductive elimination reactions (the reverse reaction of oxidative addition).[2−11]

The oxidative addition to a d^{10} metal complex, $M(PR_3)_2$ (M = Pd or Pt), was theoretically investigated in several works,[3a−b,4a,5,10a−c,12] probably because this reaction system is rather small and its electronic structure is not very complicated. Its transition state (TS) was considered planar in those works, according to the elegant analysis of orbital interaction that participates in the oxidative addition and the reductive elimination,[13] as follows: Since the charge transfer (CT) to an X−Y σ^* orbital (X, Y = H, C, or Si) from a metal d orbital is necessary to break the X−Y bond and to form M−X and M−Y bonds, the X−Y σ^* orbital should overlap well the occupied d_π orbital that is at a high energy. As shown in Scheme 1, the d_{xz} orbital is at a higher energy than the other d orbitals, because the d_{xz} orbital which lies on the PtP_2 plane undergoes antibonding mixing of the lone pair orbital of PR_3 but the other d orbitals do not undergo such antibonding mixing. Thus, the d_{xz} orbital can form more strongly the CT interaction with X−Y σ^* orbital than does the d_{yz} orbital, and the TS must be planar, to yield a good overlap between X−Y σ^* and d_{xz} orbitals. Actually, Obara et al. theoretically investigated the H−H oxidative addition to $Pt(PH_3)_2$ and reported that its TS was planar and a nonplanar TS which was optimized under a constraint of a pseudo-tetrahedral structure exhibited two imaginary frequencies and therefore it was not a true TS.[3b]

SCHEME 1

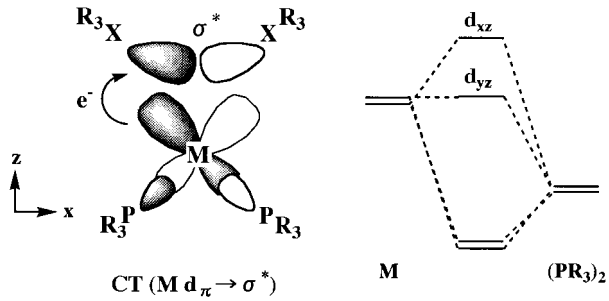

However, the nonplanar TS structure was reported recently in the oxidative addition of $(HO)_2B-B(OH)_2$ to $Pt(PH_3)_2$.[3g] Also, we independently found that the TS structure is nonplanar in the oxidative addition of SiH_3-CH_3 to $Pt(PH_3)_2$, recently. In the oxidative addition to a d^{10} transition metal complex, the product takes a singlet d^8 electron configuration, and therefore, they are planar, in general. The nonplanar pseudo-tetrahedral d^8 metal complex would take an open-shell triplet state. Thus, there is a need to investigate whether the nonplanar pseudo-tetrahedral TS is smoothly connected to the planar product on the singlet surface. This means that not only the frequency analysis but also the intrinsic reaction coordinate (IRC) calculation[14] should be carried out.

In this theoretical work, we reinvestigated the oxidative additions of $H-CH_3$, CH_3-CH_3, $H-SiR_3$, and SiR_3-CH_3 (R = H, Cl, or Me) to $Pt(PH_3)_2$. We selected these reactions for

* Author to whom correspondence should be addressed.
† Department of Applied Chemistry and Biochemistry.
‡ Information Processing Center.

S1089-5639(98)01899-4 CCC: $15.00
Published on Web 09/19/1998

the following reasons: (1) the Si−H oxidative addition is involved as a key step of transition-metal catalyzed hydrosilylation of alkene, which has received considerable attention in organosilicon chemistry;[1c,d] (2) the Si−C reductive elimination (the reverse reaction of the Si−C oxidative addition) is a key step to yield the product in the well-known Chalk−Harrod mechanism of transition metal-catalyzed hydrosilylation of alkene;[1c,d,15] and (3) the C−H oxidative addition is one of the attractive reactions in organometallic chemistry.[1a,b] Our main purposes are to provide a clear conclusion on the transition state (TS) structure, in particular, to investigate what reaction takes place through a nonplanar TS and what reaction through a planar TS, to elucidate whether the nonplanar TS smoothly leads to the planar product on the singlet surface if the TS is nonplanar, and also to present a detailed understanding of the Si−C oxidative addition, since oxidative addition and reductive elimination of the Si−C σ-bond have been subjects of recent interest.[15,16]

Computational Details

Geometries were optimized with the ab initio MO/MP2 method, where the geometry of PH_3 was taken from the experimental structure of a free PH_3 molecule.[17] Energy change was calculated with ab initio MO/MP4SDQ, CCD (coupled cluster with double substitutions) and CCSD (coupled cluster with single and double substitutions) methods, using the MP2-optimized geometries. In CCD calculations, the contribution of single and triple excitations was evaluated with fourth order perturbation, using CCD wave functions.[18] This method is called CCD(ST4). In CCSD calculations, triple excitations were taken into consideration noniteratively.[19] In these calculations, core orbitals were excluded from the active space.

Two kinds of basis set systems were used. In the smaller system (BS I), core electrons of Pt (up to 4f) and P (up to 2p) were replaced with effective core potentials (ECPs),[20,21] and their valence electrons were represented with (311/311/21) and (21/21) sets,[20,21] respectively. The MIDI-3 basis set of Huzinaga et al. was employed for C and Si atoms,[22] where a d-polarization function[23] was added to Si. The usual (31) set was used for H,[23] where a p-polarization function was added to a hydride and the active H atom of CH_4 and $SiHR_3$ that turns into a hydride through the oxidative addition reaction. In the larger system (BS II), the same ECPs as those in BS I were employed for core electrons of Pt and P atoms,[20,21] respectively, while a slightly more flexible (311/311/111) set was adopted for valence electrons of Pt[21] and a (21/21) set for P was augmented with a d-polarization function.[21] Huzinage−Dunning (9s5p1d)/[3s2p1d][23] and (12s8p1d)/[6s4p1d] sets[23] were employed for C and Si, respectively. The (31/1) set[23] was used for H except for H of PH_3 which was represented with the (31) set. Gaussian 92 and 94 programs[24] were used.

Results and Discussion

Geometry Changes. In oxidative addition reactions of CH_4 and SiH_4, geometry changes are essentially the same as those of previous investigations,[10a−c] as shown in Figure 1. In the reactions of CH_3-CH_3 and SiH_3-CH_3, however, the transition state (TS) structures are nonplanar, as shown in Figures 2 and 3.[25] In the TS, the dihedral angle (δ) between PtP_2 and PtXC planes (X = C or Si) is about 80° for X = C and about 70° for X = Si. For the purpose of a comparison, a planar TS geometry was optimized under a constraint of C_s symmetry. This planar TS is represented here by (TS_{pl}) with a parenthesis to show that this is not a real TS (vide infra). It is noted here that the intermolecular distance between Pt and a substrate (SiH_3-CH_3 and CH_3-CH_3) is much longer in (TS_{pl}) than that in the nonplanar TS. This significant difference between TS and (TS_{pl}) will be discussed below.

To clarify whether the TS structure depends on substituents, oxidative additions of $H-SiR_3$ and SiR_3-CH_3 (R = Cl or Me) were investigated too. As clearly shown in Figure 4, the TS of the $H-SiR_3$ reaction is planar, while the TS of the SiR_3-CH_3 (R = Cl or Me) reaction is nonplanar; the dihedral angle δ is 76° for $SiMe_3-CH_3$ and 84° for $SiCl_3-CH_3$. These dihedral angles are much larger than that in the TS of SiH_3-CH_3 oxidative addition, which will be discussed below in more detail.

All the products were calculated to be planar, as expected, as shown in Figures 1−4. The calculated Pt−H (1.550 Å) and Pt−CH_3 (2.094 Å) distances of $PtH(CH_3)(PH_3)_2$ agree well with their experimental values of a similar platinum(II) complex, $PtH(CH_2Bu^t)$(dtbpm) (dtbpm = di-*tert*-butylphosphinomethane);[26] R(Pt−H) = 1.58 Å and R(Pt−C) = 2.107 Å. Of course, $PtH(CH_2Bu^t)$(dtbpm) is planar. The recently reported cis-$Pt(CH_3)(SiPh_3)(PMePh_2)_2$ is also planar.[15] The calculated Pt−$SiMe_3$ (2.367 Å) and Pt−CH_3 (2.124 Å) bond distances of cis-$Pt(CH_3)(SiMe_3)(PH_3)_2$ agree well with the experimental Pt−$SiPh_3$ (2.381 Å) and Pt−CH_3 (2.113 Å) bond distances, respectively. In $Pt(CH_3)(SiCl_3)(PH_3)_2$, however, the calculated Pt−$SiCl_3$ bond (2.280 Å) is slightly shorter and the calculated Pt−CH_3 bond (2.141 Å) is slightly longer than the corresponding experimental bond lengths. The P−Pt−P, P−Pt−C, P−Pt−Si, and Si−Pt−C angles agree well with those experimental values. However, the calculated Pt−PH_3 distance is somewhat longer than the experimental value even after considering several differences between model and real compounds. This disagreement would arise from the absence of d-polarization function in the P basis set used for geometry optimization. Actually, our previous study of the C−H reductive elimination of $Pd(H)(\eta^3-C_3H_5)(PH_3)$[27] indicated that the P basis set without a d-polarization function yields a longer Pd−P distance than the usual experimental Pd−P bond distance but addition of a d-polarization function to the P basis set shortens the Pd−PH_3 distance and the optimized Pd−P distance agrees well with the experimental value. However, the energy change in the reaction calculated with the long Pd−PH_3 distance was almost the same as that calculated with the correct Pd−PH_3 distance. In $Pt(CH_3)(SiH_3)(PH_3)_2$, the calculated Pt−P(2) bond at the position trans to the silyl ligand is 0.08 Å longer than the Pt−P(1) bond at the position trans to the alkyl ligand like those in the real compound, cis-$Pt(CH_3)(SiPh_3)(PMePh_2)_2$,[15] in which the Pt−P(2) distance is 0.07 Å longer than the Pt−P(1) bond. The above results suggest that the model system, $Pt(PH_3)_2$, is not unsuitable for the investigation of oxidative addition reactions and the energy change calculated for the present model would be little influenced by the long Pt−PH_3 distance.

We will mention here geometries of the precursor complexes. In all the precursor complexes, $Pt(PH_3)_2$ and substrates show little distortion, which indicates that the interaction between them is very weak, as previously discussed.[10] There are several possible structures in the precursor complex of SiR_3-CH_3; in the first (**PCa** in Figure 2), the Si−C bond is almost parallel to the *z*-axis and the SiR_3 group interacts with Pt similarly to the precursor complex of SiH_4, in the second (**PCb** in Figure 2), the Si−C bond is almost perpendicular to the *z*-axis, and in the third, the CH_3 group interacts with Pt similarly to the precursor complex of CH_4 (see Figure 1). Since the third one was previously calculated to be less stable than the first and the second ones when R = H,[10b] we examined here the first and

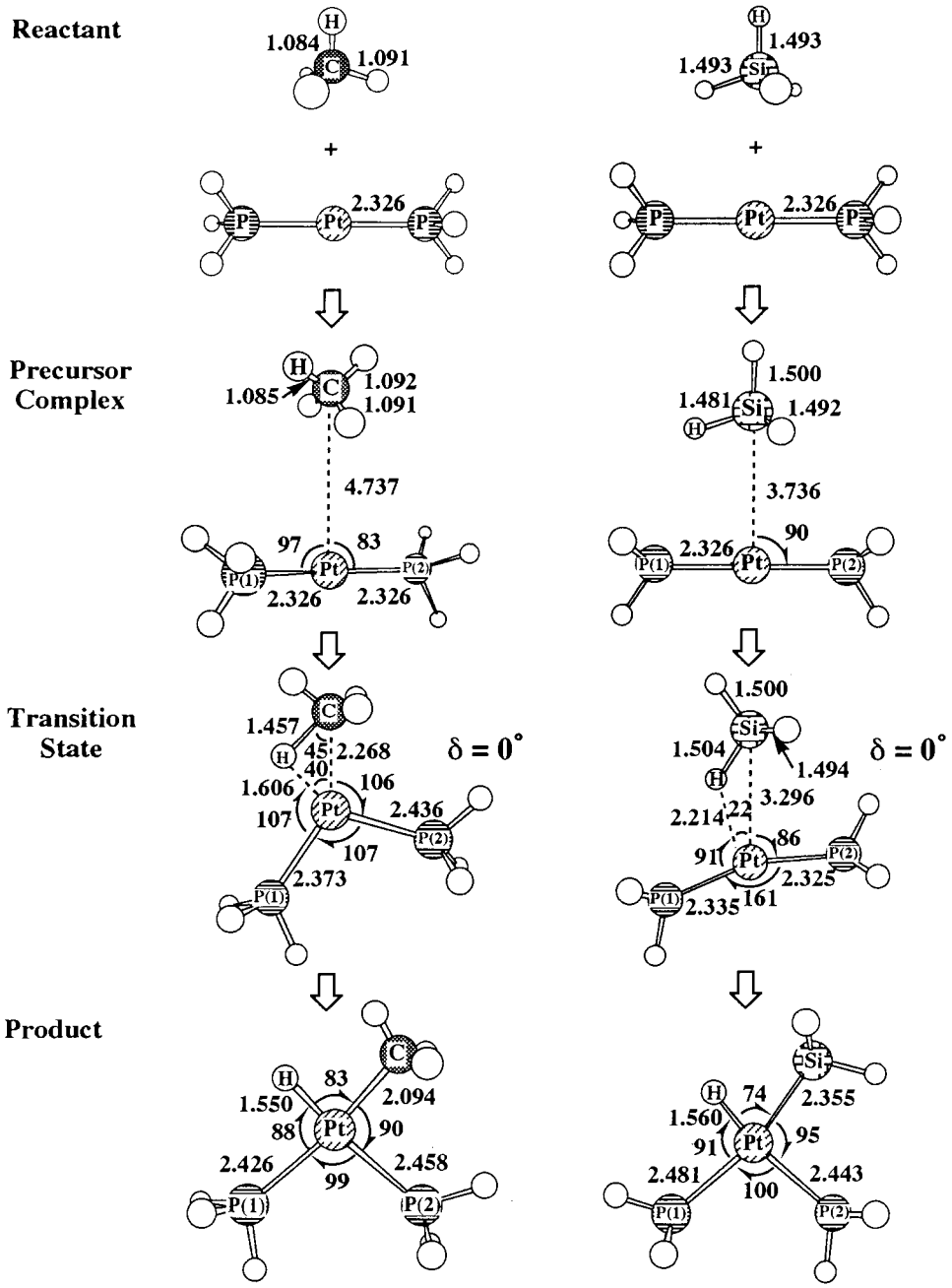

Figure 1. Geometry changes in the oxidative additions of H−CH_3 and H−SiH_3 to $Pt(PH_3)_2$. Bond length in Å and bond angle in degrees.

the second structures. When R = Me, **PCb** is more stable than **PCa** by ca. 0.6 kcal/mol (MP4SDQ values are given hereafter). When R = H, **PCa** is slightly more stable than **PCb** by 0.7 kcal/mol for R = H, but **PCa** is considered to be a precursor complex for the Si−H oxidative addition. In **PCb**, the orientation of the Si−C bond is different from the TS. However, the Si−C bond easily rotates around the *z*-axis, since the interaction between Pt and SiR_3−CH_3 is very weak (vide infra). Thus, **PCb** is considered to be on the reaction course, and the activation energy was evaluated as an energy difference between **PCb** and the TS when R = H or Me. When R = Cl, **PCb** could not be successfully optimized and the geometry gradually changed into **PCa**. This suggests that **PCb** cannot exist even in a local minimum. Thus, the activation energy was defined as an energy difference between the TS and **PCa**, in R = Cl. In the precursor complex of CH_3−CH_3, we also examined two structures; in one (**PCa** in Figure 3), the CH_3 group approaches Pt in a similar way to the precursor complex of CH_4, and in the other (**PCb** in Figure 3), the C−C bond is almost perpendicular to the *z*-axis. The former is slightly more stable than the latter by 2.2 kcal/mol, and it is considered to be on the reaction course.

Frequency Analysis of the Transition State and IRC Calculation. To investigate whether the calculated TS is true, the frequency analysis was carried out at the MP2 level. In the TS of Si−H oxidative addition, one imaginary frequency of 93i cm^{-1} was calculated. The eigenvector corresponding to this imaginary frequency is schematically shown in Figure 5a; the H^1 atom takes a position nearer to Pt than the Si atom, and both H^1 and Si atoms are approaching Pt. At the same time, the SiH_3 group is changing its direction toward Pt. In the TS of SiH_3−CH_3 oxidative addition, one imaginary frequency of 224i cm^{-1} was calculated. Its eigenvector is shown in Figure 5b; both C and Si atoms are approaching Pt with a slight lengthening of the Si−C bond. At the same time, SiH_3 and CH_3 groups are changing their directions toward Pt. In (TS_{pl}) of the SiH_3−CH_3 oxidative addition, however, two imaginary

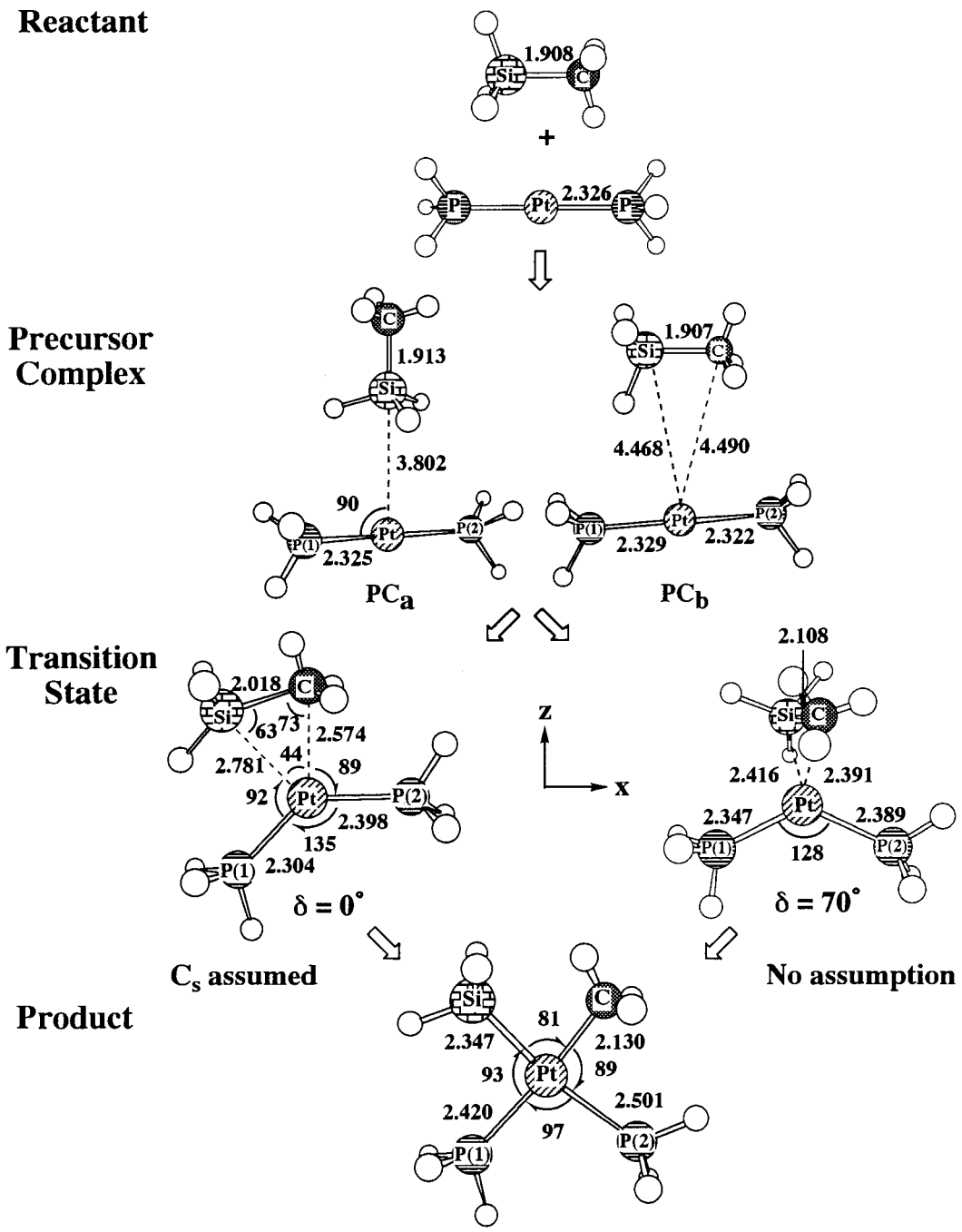

Figure 2. Geometry changes in the oxidative addition of SiH_3-CH_3 to $Pt(PH_3)_2$. Bond length in Å and bond angle in degrees. The planar transition state was optimized under a constraint of the C_s symmetry.

frequencies (265i and 158i cm^{-1}) were calculated (Figure 5c). The eigenvector corresponding to the former frequency involves the Si−C bond breaking and the Pt−Si and Pt−C bond formation, but the eigenvector corresponding to the latter one involves the tilts of SiH_3 and CH_3 groups. These results clearly show that the nonplanar TS is a true TS but (TS_{pl}) is not true.

Although the frequency analysis elucidated that the nonplanar TS of Si−C oxidative addition involves only one imaginary frequency, we carried out an IRC calculation to ascertain that this nonplanar TS is smoothly connected to the planar product.[28] As shown in Figure 6, the total energy of the system is gradually lowered, as SiH_3-CH_3 approaches Pt after the TS. However, the dihedral angle between PtSiC and PtP_2 planes changes little until the Pt−Si and Pt−C distances become similar to those of the product, but the dihedral angle starts to decrease when the Pt−Si and Pt−C distances become about 2.3 and 2.2 Å, respectively, and the Si−C distance lengthens to about 2.6 Å, as shown in Figure 6. These bond distances suggest that the Pt−Si and Pt−C bonds are almost formed and the Si−C bond is almost broken at this structure. One important feature to be noted is that Pt−P(1) and Pt−P(2) distances become longer after the TS, as the Pt−Si and Pt−C distances become shorter and the geometry becomes similar to that of the product. The Pt−P(1) and Pt−P(2) bond lengthening leads to stabilization of the singlet state, as follows: When the Si−C bond is broken and the Pt−Si and Pt−C bonds are formed, the central metal is considered to take a d^8 electron configuration in a formal sense. If the Pt−P(1) and Pt−P(2) distances were short, the d_{xz} orbital was destabilized in energy like the d_{yz} orbital, as shown in Scheme 2, and therefore, the triplet state became stable. However, since the Pt−P(1) and Pt−P(2) bonds lengthen, the d_{xz} orbital becomes more stable in energy than the d_{yz} orbital,

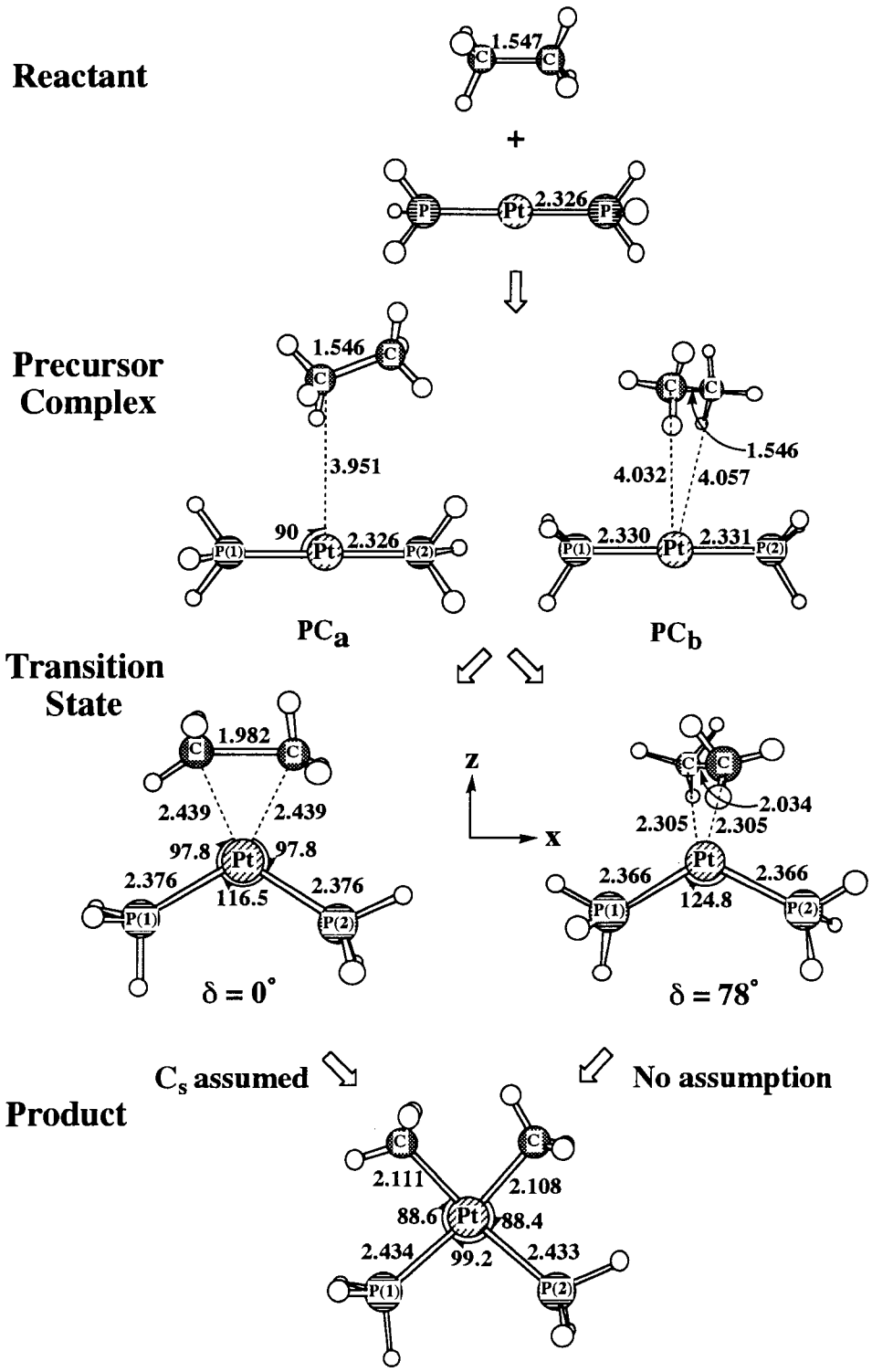

Figure 3. Geometry changes in the oxidative addition of CH_3-CH_3 to $Pt(PH_3)_2$. Bond length in Å and bond angle in degrees. The planar transition state was optimized under a constraint of the C_s symmetry.

and the singlet state would become more stable than the triplet state. Actually, the triplet state is calculated to be 104 kcal/mol less stable than the singlet state at the TS, where the UMP2/BS I calculation was carried out.[29]

We briefly examined the IRC calculation going to the reactant side. As SiH_3-CH_3 is eliminated from Pt, the dihedral angle δ decreases. This means that the geometry approaches the precursor complex in which the Si−C bond is parallel to the P−Pt−P axis. Thus, the nonplanar TS is smoothly connected to both the planar product and the precursor complex.

From the above results, a coherent picture of the Si−C oxidative addition might emerge as follows; In the precursor complex, the Si−C bond is parallel to the P−Pt−P axis. Then, SiH_3-CH_3 approaches $Pt(PH_3)_2$ with changing orientation and lengthening of the Si−C bond. At the TS, the Si−C bond is almost perpendicular to the PtP_2 plane. After the TS, the dihedral angle δ starts to decrease, when Pt−Si and Pt−C distances become short like those of the product. At the same time, the Pt−P(1) and Pt−P(2) bonds somewhat lengthen to stabilize the singlet state relative to the triplet state; in other

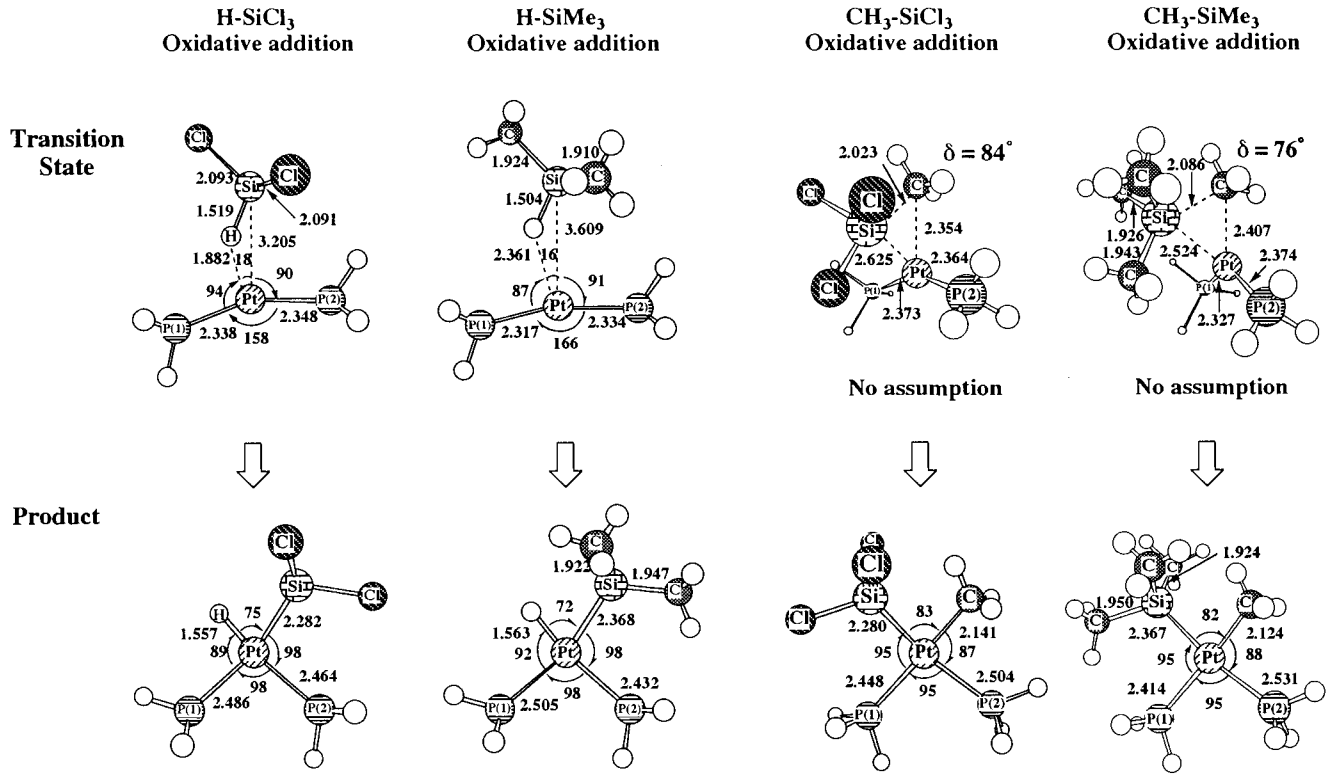

Figure 4. Geometries of transition state and product of the oxidative addition of $H-SiR_3$ and SiR_3-CH_3 (R = Cl or Me) to $Pt(PH_3)_2$. Bond length in Å and bond angle in degrees.

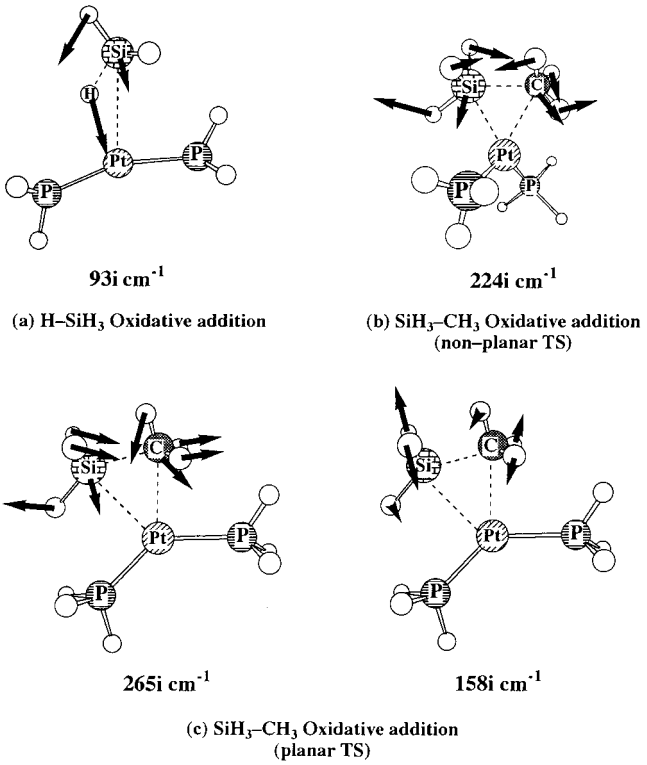

Figure 5. Schematic picture of reaction coordinate vectors at the transition state.

words, the Pt−P(1) and Pt−P(2) bond lengthening is necessary to reach the product on the singlet surface.

Activation Energy (E_a) and Reaction Energy (ΔE). BE, E_a, and ΔE are calculated with various computational methods, where BE is the energy difference between the precursor complex and the sum of reactants, E_a is the energy difference between the TS and the precursor complex, and ΔE is the energy difference between the product and the sum of reactants. A negative value represents stabilization in energy. Introduction of electron correlation decreases E_a very much, as expected, and also decreases ΔE (i.e., increases the exothermicity), as shown in Table 1. BE, E_a, and ΔE change little upon going from MP4DQ to CCSD(T), while E_a and ΔE fluctuate moderately around MP2 and MP3 levels. Thus, a comparison among various oxidative additions examined here would be made reliably with the MP4SDQ method. We mention here that BE is very small, consistent with the fact that both SiR_3-CH_3 and $Pt(PH_3)_2$ moieties distort little in the precursor complex.

As shown in Table 2, (TS_{pl}) is much less stable in energy than the real TS by about 7 to 13 kcal/mol in SiR_3-CH_3 oxidative addition reactions and by about 6 kcal/mol in CH_3-CH_3 oxidative addition reaction. This result is consistent with the finding that (TS_{pl}) exhibits two negative frequencies, as discussed above.

Several interesting results are found in Table 2; for instance, (1) the C−H oxidative addition requires a higher E_a than the Si−H oxidative addition, (2) the CH_3-CH_3 oxidative addition needs a much higher E_a than the $H-CH_3$ oxidative addition, whereas the reaction energy is similar in these two reactions, and (3) the SiR_3-CH_3 oxidative addition needs a higher E_a than the $H-SiR_3$ oxidative addition, and the former reaction is less exothermic than the latter one. Result (1) is easily understood by considering that the Si−H bond is weaker than the C−H bond and the $Pt-SiH_3$ bond is stronger than the $Pt-CH_3$ bond.[10a] Results (2) and (3) are easily explained in terms of a spherical 1s orbital of H and a directional sp^3 valence orbitals of CH_3 and SiR_3, as follows:[5b−c,30,31] The H atom can form a new Pt−H bond without significant weakening of C−H and Si−H bonds since the H 1s orbital is spherical. This feature corresponds to the two-electron three-center interaction of the H atom. On the other hand, SiR_3 and CH_3 must change their

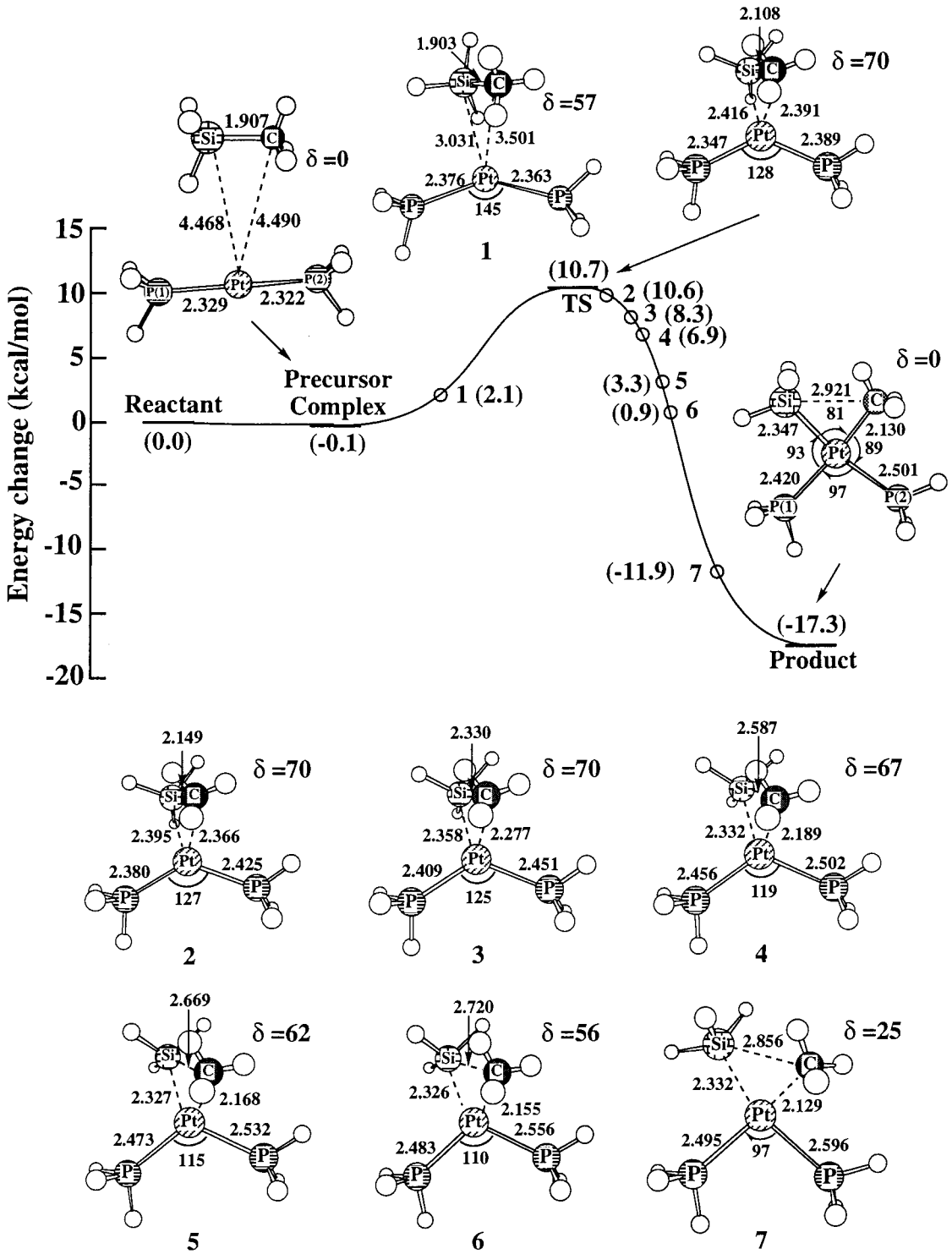

Figure 6. Changes of total energy and geometry by IRC calculation of the SiH_3-CH_3 oxidative addition to $Pt(PH_3)_2$. Intrinsic reaction coordinate calculation was carried out with the MP2/BS−I method, where the energy zero was taken for the sum of reactants.

direction toward Pt to form a bonding interaction with Pt, because of their directional sp^3 valence orbital. This geometry change causes the Si−C and C−C bond weakening. Thus, the C−C and Si−C oxidative additions require a higher E_a than the C−H and Si−H oxidative addition reactions, respectively.

The other important feature to be noted is that E_a of the H−SiR_3 oxidative addition depends little on the substituent, while ΔE depends significantly on the substituent (see Table 2). This is because the TS is very reactant-like, as shown in Figures 1 and 4. In other words, the bond strength in the product has little influence on the TS stability. On the other hand, E_a of SiR_3-CH_3 oxidative addition depends on the substituent, as shown in Table 2; E_a is lowered in the order R = Me > H > Cl, and the reaction becomes more exothermic in the same order. In this reaction, TS is not reactant-like but intermediate between the reactant and the product. Thus, the TS stability is influenced by the stability of products; in other words, the E_a order is related to the stability order of the product.

Reasons for the Nonplanar TS in the Si−C and C−C Oxidative Addition Reactions. Electron distribution would reflect the bonding nature of planar and nonplanar TS structures. In Table 3, natural bond orbital (NBO) populations[32] are

SCHEME 2: Orbital Interaction Diagram in a d^8 System with a Pseudo-tetrahedral Structure

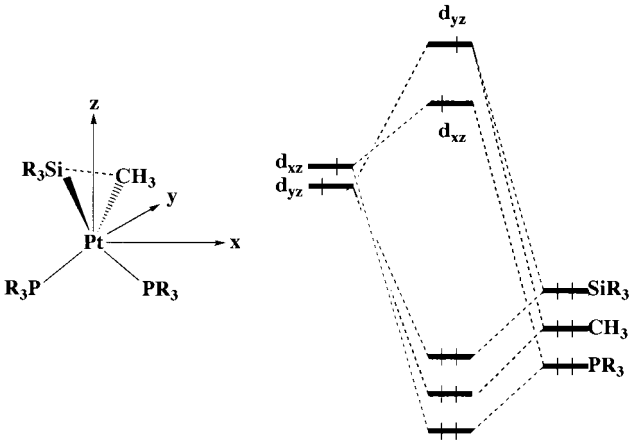

TABLE 1: Binding Energy (BE), Activation Energy (E_a), and Reaction Energy (ΔE) of SiH_3-CH_3 Oxidative Addition to $Pt(PH_3)_2$, in kcal/mol

	BE[a]	E_a[b]	ΔE[c]
HF	0.6	42.1	11.7
MP2	−2.3	16.2	−10.4
MP3	−2.2	24.8	−5.9
MP4DQ	−2.0	21.9	−6.5
MP4SDQ	−2.3	19.5	−7.1
CCD(ST4)	−2.5	19.5	−7.3
CCSD(T)	−2.5	20.1	−8.5

[a] $BE = E_t\{Pt(PH_3)_2\} + E_t(SiH_3{-}CH_3) - E_t$(precursor complex). A negative value represents the stabilization of the precursor complex relative to reactants. [b] $E_a = E_t(TS) - E_t$(precursor complex). [c] $\Delta E = E_t$(product) $- E_t\{Pt(PH_3)_2\} - E_t(SiH_3{-}CH_3)$.

TABLE 2: Activation Energy (E_a) and Reaction Energy (ΔE) of Various Oxidative Additions Examined; MP4SDQ/BS II Calculation (kcal/mol)

substrates	E_a[a]	ΔE[b]
$H{-}CH_3$	27.9	9.4
$CH_3{-}CH_3$	57.4 (63.2)[c]	7.6
$H{-}SiH_3$	2.9	−19.3
$H{-}SiCl_3$	3.0	−16.8
$H{-}SiMe_3$	2.8	−32.3
$SiH_3{-}CH_3$	19.5 (27.6)[c]	−7.1
$SiCl_3{-}CH_3$	15.5 (28.1)	−12.8
$SiMe_3{-}CH_3$	23.2 (34.6)	−2.8

[a] $E_a = E_t(TS) - E_t$(precursor complex). [b] $\Delta E = E_t$(product) $- E_t\{Pt(PH_3)_2\} - E_t$(substrate). [c] In parentheses: $E_t\{(TS)_{pl}\} - E_t$(precursor complex).

compared between $\delta = 0°$ and 90°, where the other geometrical parameters were taken to be the same as those of $(TS)_{pl}$. Apparently, the d_{xz} orbital population of the planar structure ($\delta = 0°$) is smaller than the d_{yz} orbital population of the nonplanar structure ($\delta = 90°$) in both C−C and Si−C oxidative additions. Since the d_{xz} orbital is mainly involved in the CT interaction with X−Y σ^* orbital in the planar structure and the d_{yz} orbital is mainly involved with it in the nonplanar structure (see Figures 2 and 3 for *x*-, *y*-, and *z*-axes), the above-mentioned electron distribution indicates that the d_{xz} orbital can form a stronger CT interaction with $SiH_3{-}CH_3$ in the planar $(TS)_{pl}$ than does the d_{yz} orbital in the nonplanar TS. This result is consistent with the expectation from the orbital interaction diagram, as discussed in ref 13, because the d_{xz} orbital is at a higher energy than the d_{yz} orbital, as shown in Scheme 1. Thus, it is reasonably concluded that the planar TS is more favorable on the basis of the electronic factor and the reason for nonplanar TS cannot be attributed to the electronic factor.

TABLE 3: Comparison of NBO Populations between 0° and 90° of Dihedral Angle[a]

	$CH_3{-}CH_3$		$SiH_3{-}CH_3$	
	(TS_{pl})	90°	(TS_{pl})	90°
Pt	78.089	78.025	78.211	78.214
d	9.441	9.384	9.498	9.504
d_{xz}	1.807	1.851	1.830	1.902
d_{yz}	1.949	1.824	1.962	1.911
$XH_3{-}CH_3$ (X = C or Si)	18.114	18.163	26.114	26.078

[a] The structure of $\delta = 0°$ was taken to be the same as that of (TS_{pl}), and the structure of 90° was taken to be the same as that of (TS_{pl}) without only the dihedral angle (δ) between PtP_2 and PtXC planes.

The remaining factor is a steric repulsion between phosphine and substrate. Actually, the dihedral angle δ is 0° for small substrates such as $H{-}CH_3$ and $H{-}SiR_3$. In these substrates, the steric repulsion is essentially small even when $\delta = 0°$. Moreover, the steric repulsion is similar between $\delta = 90°$ and $\delta = 0°$, since these substrates approach Pt with H in a lead at their TS and the CH_3 and SiR_3 groups are much more distant from Pt than H (see Figure 1). On the other hand, the dihedral angle δ is 70° for bulky $SiH_3{-}CH_3$, and 76° and 84° for more bulky $SiMe_3{-}CH_3$ and $SiCl_3{-}CH_3$, respectively. The Pt−Si distance also seems to reflect the steric repulsion; it is 2.42 Å for $SiH_3{-}CH_3$, 2.52 Å for $SiMe_3{-}CH_3$, and 2.63 Å for $SiCl_3{-}CH_3$. One plausible explanation is that a bulky SiR_3 group leads to a long Pt−Si distance, and at the same time, a large dihedral angel δ. Also, the longer Pt−($SiR_3{-}CH_3$) and Pt−($CH_3{-}CH_3$) distances in (TS_{pl}) than those in the nonplanar TS would arise from the larger steric repulsion between $Pt(PH_3)_2$ and the substrate in (TS_{pl}) than that in the nonplanar TS.

From the above discussion, it is reasonably concluded that (1) the electronic factor favors the planar TS, and (2) a steric factor is responsible for the nonplanar TS structure.

Electronic Process in the $SiH_3{-}CH_3$ Oxidative Addition. Since the Si−C reductive elimination (the reverse of Si−C oxidative addition) is involved as a key step in the transition metal catalyzed hydrosilylation of alkene,[1c] this reductive elimination has received recent attention in the experimental field.[15] Here, we discuss the characteristic features of the Si−C oxidative addition, in an attempt to show how to facilitate Si−C oxidative addition (and Si−C reductive elimination).

As shown in Figure 7, the Pt atomic population decreases and the SiH_3 population increases, as expected, as the Si−C oxidative addition proceeds. The decrease of the Pt atomic population arises from the decrease of the Pt d orbital population. These results are consistent with the understanding that this is the oxidative addition reaction. However, the CH_3 population unexpectedly slightly decreases. This unexpected feature is interpreted in terms of electronegativities of C and Si atoms; since the C atom is more electronegative than the Si atom, the C atom has enough electron population in $SiR_3{-}CH_3$, and therefore, the C atom does not need to receive electron population from the Pt atom. Thus, the C atomic population slightly decreases in the Si−C oxidative addition. On the other hand, the Si atom is short of electron population in $SiR_3{-}CH_3$. As a result, its electron population increases when it interacts with the Pt atom, because the Pt atom is more electropositive than the Si atom.

The other important feature is that the Pt d orbital population starts to decrease significantly after TS. This result clearly indicates that the charge-transfer (CT) from Pt to $SiH_3{-}CH_3$

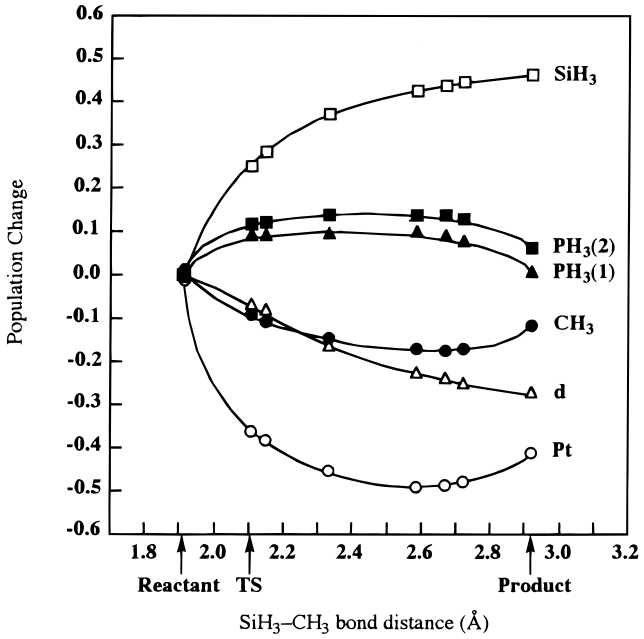

Figure 7. NBO population changes in the SiH_3-CH_3 oxidative addition to $Pt(PH_3)_2$. A positive value means an increase in the population and vice versa.

TABLE 4: Distortion Energies (kcal/mol)[a] of SiR_3-CH_3 and $Pt(PH_3)_2$

	TS	(TS_{pl})
(a) SiH_3-CH_3 oxidative addition		
SiH_3-CH_3	24.6	20.6
$Pt(PH_3)_2$	14.2	10.6
(b) $SiMe_3-CH_3$ oxidative addition		
$SiMe_3-CH_3$	24.4	26.3
$Pt(PH_3)_2$	11.7	16.3
(c) $SiCl_3-CH_3$ oxidative addition		
$SiCl_3-CH_3$	42.0	32.1
$Pt(PH_3)_2$	5.8	9.2

[a] MP4/BS II calculation.

which is necessary to break the Si−C bond does not occur effectively at the TS. This feature is consistent with the fact that the Si−C bond lengthens by only 0.2 Å and therefore it is not completely broken at the TS. However, this does not mean that the Si−C bond breaking is not responsible for the origin of the activation barrier.

At the TS, not only does the Si−C bond lengthen by 0.2 Å but also the SiH_3 and CH_3 groups tilt considerably from the equilibrium structure by 27° and 20°, respectively, which shows that the Si−C bond weakening already starts at the TS. Actually, SiH_3-CH_3 taking the distorted structure like that in TS provides a considerable distortion energy, and its distortion energy is much larger than that of $Pt(PH_3)_2$ in both (TS_{pl}) and TS, as shown in Table 4. Thus, the SiR_3-CH_3 distortion considerably contributes to the activation barrier. Although the CT interaction between Si−C σ^* and Pt d_{yz} orbitals is not yet formed at the TS, SiR_3-CH_3 makes a preparation to form the CT interaction between Si−C σ^* and Pt d_{yz} orbitals at the TS. Since the Pt d_{yz} orbital is not destabilized in energy by the phosphine lone pair orbital (see Scheme 1), the energy lowering of the Si−C σ^* orbital is necessary to form effectively the CT interaction. This requires the considerable distortion of SiR_3-CH_3, which corresponds to the considerable weakening of the Si−C bond in the nonplanar TS. The above discussion leads to a conclusion that the E_a in the nonplanar TS arises mainly from the SiR_3-CH_3 bond weakening and secondarily from the $Pt(PH_3)_2$ distortion which would be induced by the steric repulsion with the substrate.

SCHEME 3: Back Bonding from Pt d to Alkyne π^*

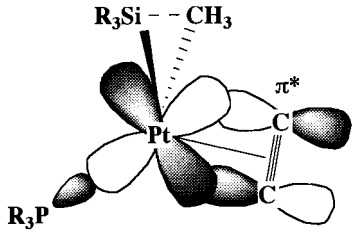

It is important to find conditions which stabilize the TS of Si−C oxidative addition. At the present stage, we do not have a concrete conclusion, but we might propose several factors to stabilize the TS of the Si−C oxidative addition. One is the use of a small phosphine, to reduce the steric repulsion between phosphine and substrate. The donating ability of the phosphine seems not to be very important, because the phosphine lone pair orbital does not overlap well with the d_{yz} orbital which interacts with the Si−C σ^* orbital at the TS. The other is to use a phosphine that is favorable for the decrease of P−Pt−P angle, since the P−Pt−P angle must decrease at the TS probably to reduce the steric repulsion with substrate. This means that a strongly coordinating phosphine is not favorable. These considerations suggest that phosphite is one of the candidates for a good ligand. In particular, $P(OCH_2)_3CEt$ is considered very good, since the cone angle is small and its donating ability seems weak. Actually, this phosphite was successfully used as a ligand in Pt-catalyzed double silylation of alkyne and α-diketone,[33] in which the Si−Si oxidative addition and the Si−C reductive elimination would be involved.

The above discussion also provides us a reasonable understanding of the recent experimental report that the Si−C reductive elimination from cis-$Pt(CH_3)(SiPh_3)(PMePh_2)_2$ is difficult but the reductive elimination of cis-$Pt(CH_3)(SiPh_3)(PMePh_2)(RC{\equiv}CR)$ easily takes place.[15] At the TS, the $Pt(PR_3)(RC{\equiv}CR)$ moiety would bend like the $Pt(PR_3)_2$ moiety. In such a bending structure, an electron-withdrawing alkyne can stabilize the TS through the back-bonding interaction with the Pt d orbital that is destabilized by the antibonding overlap with the lone pair of PR_3, as shown in Scheme 3. On the other hand, phosphine cannot effectively form the π-back-bonding interaction, because of the lack of a good acceptor orbital. Thus, the TS of Si−C oxidative addition (and Si−C reductive elimination) would be more stable in $Pt(SiR_3-CH_3)(PR_3)(RC{\equiv}CR)$ than in $Pt(SiR_3-CH_3)(PR_3)_2$, and the Si−C reductive elimination is accelerated by substitution of PR_3 by an electron-withdrawing alkyne, as reported experimentally.[15]

Conclusions

Oxidative additions of $H-CH_3$, CH_3-CH_3, $H-SiR_3$, and SiR_3-CH_3 to $Pt(PH_3)_2$ were theoretically investigated with ab initio MO/MP2-MP4SDQ, CCD, and CCSD methods. In this work, we put our main focus on the transition state structure, in particular, whether TS is planar or not. The TS structure of $H-CH_3$ and $H-SiR_3$ oxidative additions is planar, in accordance with the orbital interaction diagram. On the other hand, the TS structure of the CH_3-CH_3 and SiR_3-CH_3 oxidative additions is nonplanar, not our expectation from an orbital interaction diagram. Frequency analysis and IRC calculations clearly indicate that this nonplanar TS is a real TS and that the nonplanar TS is smoothly connected to the planar product on the singlet surface. The electron distribution suggests that the

planar structure involves the stronger CT interaction from Pt d orbital to Si−C and C−C σ^* orbital than does the nonplanar structure. This means that the electronic factor is not responsible for the nonplanar TS. Moreover, the dihedral angle δ between the PtP_2 plane and the Si−C bond increases in the order SiH_3-CH_3 < $SiMe_3-CH_3$ < $SiCl_3-CH_3$, and the Pt−Si distance at the TS becomes longer in this order. One plausible explanation for this result is that the greater steric repulsion by the SiR_3 group leads to the longer Pt−SiR_3 distance and the larger dihedral angle δ. Thus, it is reasonably concluded that the steric factor between substrate and phosphine is responsible for the nonplanar TS structure. In other words, the planar TS is more favorable than the nonplanar TS as a result of the electronic factor, but the nonplanar TS is more favorable than the planar TS as a result of the steric factor. If the steric repulsion is small and/or similar in both planar and nonplanar structures, the TS structure becomes planar to favor the electronic factor like those of the H−CH_3 and H−SiR_3 oxidative additions. However, if the steric factor is more important than the electronic factor, the TS becomes nonplanar to decrease the steric repulsion.

Acknowledgment. This work was financially supported by Grant-in-Aids for Scientific Research on Priority Areas "The Chemistry of Inter-Element Linkage" (No. 09239104) from the Ministry of Education, Science, Sports, and Culture, Japan. Computations were carried out with IBM RS-6000 workstations of our laboratory and an IBM-SP2 of the Institute for Molecular Science (Okazaki, Japan).

References and Notes

(1) For example: (a) Shilov, A. E. *Activation of Saturated Hydrocarbons by Transition Metal Complexes*, D. Reidel Publishing: Dordrecht, The Netherlands, 1984. (b) Still, J. K. In *The Chemistry of Metal−Carbon Bond*; Hartley, F. R., Patai, S., Eds.; John Wiley & Sons: New York, 1985; Vol. 2, p 625. (c) Tilley, T. D. In *The Chemistry of Organic Silicon Compounds*; Patai, S., Rappoport, Z., Eds.; John Wiley & Sons: New York, 1989; p 1415. (d) Ozima, I. In *The Chemistry of Organic Silicon Compounds*; Patai, S., Rappoport, Z., Eds.; John Wiley & Sons: New York, 1989; p 1479.

(2) Koga, N.; Morokuma, K. *Chem. Rev.* **1991**, *91*, 823.

(3) (a) Kitaura, K.; Obara, S.; Morokuma, K. *J. Am. Chem. Soc.* **1981**, *103*, 2891. (b) Obara, S.; Kitaura, K.; Morokuma, K. *J. Am. Chem. Soc.* **1984**, *106*, 7482. (c) Koga, N.; Morokuma, K. *J. Phys. Chem.* **1990**, *94*, 5454. (d) Koga, N.; Morokuma, K. *J. Am. Chem. Soc.* **1993**, *115*, 6883. (e) Musaev, D. G.; Morokuma, K. *J. Am. Chem. Soc.* **1995**, *117*, 799. (f) Matsubara, T.; Maseras, F.; Koga, N.; Morokuma, K. *J. Phys. Chem.* **1996**, *100*, 2573. (g) Cui, Q.; Musaev, D. G.; Morokuma, K. *Organometallics* **1997**, *16*, 1355.

(4) (a) Noell, J. O.; Hay, P. J. *J. Am. Chem. Soc.* **1982**, *104*, 4578. (b) Hay, P. J.; Chem. Phys. Lett. **1984**, *103*, 456.

(5) (a) Low, J. J.; Goddard, W. A. *J. Am. Chem. Soc.* **1984**, *106*, 6928. (b) Low, J. J.; Goddard, W. A. *J. Am. Chem. Soc.* **1986**, *108*, 6115. (c) Low, J. J.; Goddard, W. J. *Organometallics* **1986**, *5*, 609.

(6) (a) Blomberg, M. R. A.; Siegbahn, P. E. M.; Nagashima, U.; Wennerberg, J. *J. Am. Chem. Soc.* **1991**, *113*, 424. (b) Svensson, M.; Blomberg, M. R. A.; Siegbahn, P. E. M. *J. Am. Chem. Soc.* **1991**, *113*, 7076. (c) Blomberg, M. R. A.; Siegbahn, P. E. M.; Svennsson, M. *J. Am. Chem. Soc*. **1992**, *114*, 6095. (d) Siegbahn, P. E. M.; Blomberg, M. R. A. *J. Am. Chem. Soc.* **1992**, *114*, 10548. (e) Siegbahn, P. E. M. *Chem. Phys. Lett.* **1993**, *205*, 290. (f) Jensen, V. R.; Siegbahn, P. E. M. *Chem. Phys. Lett.* **1993**, *212*, 353. (g) Siegbahn, P. E. M. *J. Am. Chem. Soc.* **1993**, *115*, 5903. (h) Siegbahn, P. E. M.; Blomberg, M. R. A.; Svensson, M. *J. Am. Chem. Soc.* **1993**, *115*, 4191. (i) Blomberg, M. R. A.; Siegbahn, P. E. M.; Svensson, P. E. M. *Inorg. Chem.* **1993**, *32*, 4218. (j) Siegbahn, P. E. M.; Blomberg, M. R. A.; Svensson, M. *J. Phys. Chem.* **1993**, *97*, 2564. (k) Blomberg, M. R. A.; Siegbahn, P. E. M.; Svensson, M. *J. Phys. Chem.* **1994**, *98*, 2062. (l) Siegbahn, P. E. M.; Blomberg, M. R. A. *Organometallics* **1994**, *13*, 354. (m) Siegbahn, P. E. M. *Organometallics* **1994**, *13*, 2833. (n) Siegbahn, P. E. M. *J. Am. Chem. Soc.* **1996**, *118*, 1487.

(7) (a) Ziegler, T.; Tschinke, V.; Fan, L.; Becke, A. D. *J. Am. Chem. Soc.* **1989**, *111*, 9177. (b) Bickelhaupt, F. M.; Ziegler, T.; Schleyer, P. von R. *Organometallics* **1995**, *14*, 2289.

(8) (a) Sargent, A. L.; Hall, M. B. *Inorg. Chem.* **1992**, *31*, 317. (b) Sargent, A. L.; Hall, M. B.; Guest, M. F. *J. Am. Chem. Soc.* **1992**, *114*, 517. (c) Jimenez-Catano, R.; Hall, M. B. *Organometallics* **1996**, *15*, 189. (d) Jimenez-Catano, R.; Niu, S.; Hall, M. B. *Organometallics* **1997**, *16*, 1962.

(9) Su, M. D.; Chu, S. Y. *Organometallics* **1997**, *16*, 1621.

(10) (a) Sakaki, S.; Ieki, M. *J. Am. Chem. Soc.* **1993**, *115*, 2373. (b) Sakaki, S.; Ogawa, M.; Musashi, Y.; Arai, T. *Inorg. Chem.* **1994**, *33*, 1660. (c) Sakaki, S.; Ogawa, M.; Kinoshita, M. *J. Phys. Chem.* **1995**, *99*, 9933. (d) Sakaki, S.; Ujino, Y.; Sugimoto, M. *Bull. Chem. Soc. Jpn.* **1996**, *69*, 3047.

(11) Cundari, T. R. *J. Am. Chem. Soc.* **1994**, *116*, 340.

(12) Balazs, A. C.; Johnson, K. H.; Whitesides, G. M. *Inorg. Chem.* **1982**, *21*, 2162.

(13) Tatsumi, K.; Hoffmann, R.; Yamamoto, A.; Still, J. K. *Bull. Chem. Soc. Jpn.* **1981**, *54*, 1857.

(14) Fukui, K. *Acc. Chem. Res.* **1981**, *14*, 363.

(15) Ozawa, F.; Hikida, T.; Hayashi, T. *J. Am. Chem. Soc.* **1994**, *116*, 2844.

(16) Tanaka, Y.; Yamashita, H.; Simada, S.; Tanaka, M. *Organometallics*, **1997**, *16*, 3246.

(17) Herzberg, G. *Molecular Spectra and Molecular Structure*; Van Nostrand: Princeton, NJ, 1967; Vol. 3, p 610.

(18) Raghavachari, K. *J. Chem. Phys.* **1985**, *82*, 4607.

(19) Pople, J. A.; Head-Gordon, M.; Raghavachari, K. *J. Chem. Phys.* **1987**, *87*, 5968.

(20) Wadt, W. R.; Hay, P. J. *J. Chem. Phys.* **1985**, *82*, 285.

(21) Hay, P. J.; Wadt, W. R. *J. Chem. Phys.* **1985**, *82*, 299.

(22) Huzinaga, S.; Andzelm, J.; Klobkowski, M.; Radio-Andzelm, E.; Sakai, Y.; Tatewaki, H. *Gaussian Basis Sets for Molecular Calculations*; Elsevier: Amsterdam, 1984.

(23) Dunning, T. H.; Hay, P. J. In *Methods of Electronic Structure Theory*; Schaefer, H. F., Ed.; Plenum: New York, 1977; p 1.

(24) (a) Frisch, M. J.; Trucks, G. W.; Head-Gordon, M.; Gill, P. M. W.; Wong, M. W.; Foresman, J. B.; Johnson, B. G.; Schlegel, H. B.; Robb, M. A.; Replogle, E. S.; Gomperts, R.; Andres, J. L.; Raghavachari, K.; Binkley, J. S.; Gonzalez, C.; Martin, R. L.; Fox, D. J.; DeFrees, D. J.; Baker, J.; Stewart, J. J. P.; Pople, J. A. *Gaussian 92*, Gaussian Inc., Pittsburgh, PA, 1992. (b) Frisch, M. J.; Trucks, G. W.; Schlegel, H. B.; Gill, P. M. W.; Johnson, B. G.; Robb, M. A.; Cheeseman, J. R.; Keith, T. A.; Petersson, G. A.; Montgomery, J. A.; Raghavachari, K.; Al-Laham, M. A.; Zakrzewski, V. G.; Ortiz, J. V.; Foresman, J. B.; Cioslowski, J.; Stefanov, B. B.; Nanayakkara, A.; Challacombe, M.; Peng, C. Y.; Ayala, P. Y.; Chen, W.; Wong, M. W.; Andres, J. L.; Replogle, E. S.; Gomperts, R.; Martin, R. L.; Fox, D. J.; Binkley, J. S.; Defrees, D. J.; Baker, J.; Stewart, J. P.; Head-Gordon, M.; Gonzalez, C.; Pople, J. A. *Gaussian 94*, Gaussian, Inc.: Pittsburgh, PA, 1995.

(25) (a) In our previous work,[10a−c] we reported the planar TS, where the TS was defined without frequency calculation, by considering that one eigenvector of a Hessian matrix has a negative eigenvalue. The present calculations indicate that those planar TSs are not correct. (b) The TS of Si−Si oxidative addition to $Pt(PH_3)_2$ was optimized here, but IRC calculation failed since the system changes to the Si−H oxidative addition after the TS. We need to investigate the oxidative addition of disilane involving no Si−H bond, such as SiF_3-SiF_3. Such theoretical calculations involving IRC calculations are very time-consuming. We are planning to do it in the near future.

(26) Hofmann, P.; Heiss, H.; Neiteler, P.; Muller, G.; Lachmann, J. *Angew. Chem., Int. Ed.* **1990**, *29*, 880.

(27) Sakaki, S.; Satoh, H.; Shono, M.; Ujino, Y. *Organometallics* **1996**, *15*, 1713.

(28) The IRC calculation of the present reaction system was very time-consuming, and therefore, we could not reach the final product because of the limit of CPU time. However, we reached the geometry which gave a similar total energy as the product, as shown in Figure 6. The Pt−Si and Pt−C distances are also almost the same as those of the product, and the dihedral angle δ is 26°. These calculations are enough for our investigation since they clearly indicate that the dihedral angle decreases at the late stage of the reaction and the geometry becomes almost the same as that of the product.

(29) The triplet state calculated corresponded not to $(d_{xz})^1(d_{yz})^1$ but to $(d_{xz})^1(6p_z)^1$. Although the UHF calculation was started from the $(d_{xz})^1(d_{yz})^1$ state, the $(d_{xz})^1(6p_z)^1$ state was converged, probably because the P−Pt−P angle is rather large at the TS.

(30) Blomberg, M. R. A.; Brandemark, U.; Siegbahn, P. E. M. *J. Am. Chem. Soc.* **1983**, *105*, 5557.

(31) Saillard, J. Y.; Hoffmann, R. *J. Am. Chem. Soc.* **1984**, *106*, 2006.

(32) (a) Reed, A. E.; Weinstock, R. B.; Weinhold, F. *J. Chem. Phys.* **1985**, *83*, 735. (b) Reed, A. E.; Curtiss, L. A.; Weinhold, F. *Chem. Rev.* **1988**, *88*, 899.

(33) (a) Yamashita, H.; Catellani, M.; Tanaka, M. *Chem. Lett.* **1991**, 241. (b) Yamashita, H.; Reddy, N. P.; Tanaka, M. *Chem. Lett.* **1993**, 315. (c) Yamashita, H.; Tanaka, M. *Bull. Chem. Soc. Jpn.* **1995**, *68*, 403.